Direct computation of paths of limit points using the Asymptotic Numerical Method

Sébastien Baguet, Bruno Cochelin

IASS-IACM 2000
Fourth International Colloquium on
Computation of Shell & Spatial Structures
June 5–7, 2000
Chania – Crete, Greece

DIRECT COMPUTATION OF PATHS OF LIMIT POINTS USING THE ASYMPTOTIC NUMERICAL METHOD

S. Baguet and B. Cochelin

Laboratoire de Mécanique et d'Acoustique CNRS UPR 7051
Ecole Supérieure de Mécanique de Marseille, IMT Technopôle de Château Gombert,
13451 Marseille Cedex 20 - France
e–mail: baguet@imtumn.imt-mrs.fr

Key words: Instabilities, Fold curve, Turning points, Asymptotic Numerical Method, Extended system, Finite elements, Path following.

Abstract. *This paper is concerned with parameter dependent problems for structural instability. The aim is the direct determination of the so called fold curve connecting the limit points of the equilibrium path for a structure subjected to a variable imperfection. This is traditionally achieved by adding a well-chosen constraint equation requiring the criticality of the equilibrium. The crucial feature of the paper lies in the numerical resolution of the obtained augmented system. Indeed, it is solved using the Asymptotic Numerical Method (A.N.M.) which is well-known for its robustness. The theoretical framework upon which the A.N.M. and the extended system are based are presented. From a numerical point of view, it leads to an efficient treatment which takes the singularity of the tangent stiffness matrix into account. Emphasis is given on two specific types of geometrical imperfections. Eventually, the numerical isolation of an initial starting limit point is discussed.*

1 Introduction

As slender structures tend to be more and more widely-used, stability analysis has become an essential point in structural design today. This type of analysis is based on two main problems. The most common one concerns the determination of critical states and in particular the calculation of the maximal load that the structure can handle before loss of stability or snap-through. The second one is related to the study of the sensitivity of the structure to geometrical or material variations. Manufacture, external loadings combined with material properties can affect the perfect structure and induce such imperfections. How then does the structure behave in presence of these imperfections and how are modified the critical states ?

In the case of quasi-static linear elasticity, the governing equations of the first problem can be represented as a one-parameter system of the form

$$\boldsymbol{F}(\boldsymbol{u}, \lambda) = \boldsymbol{F}(\boldsymbol{u}) - p(\lambda) = 0 \tag{1}$$

where $\boldsymbol{F}$ stands for the internal forces, $p(\lambda)$ for the external applied loads and λ for the load parameter. The calculation of the fundamental equilibrium path of the perfect structure and the detection of the critical states along this path are commonly achieved using an incremental-iterative algorithm (Newton-like methods).

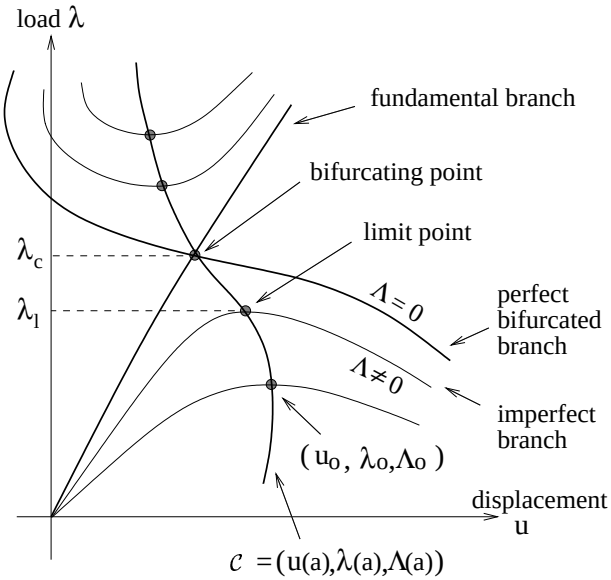

Figure 1: Perfect and imperfect equilibrium paths and limit points branch.

The second problem implies the determination of the critical states for different values of an imperfection amplitude Λ. Indeed, when a geometric (either structural or relative to the thickness) or material imperfection is introduced within the original perfect structure, the critical state can be significantly affected. Fig. 1 shows a bifurcating point becoming a limit (or turning) point with different values of Λ. As a result, this amplitude must become an additional parameter and

the system (1) becomes a two-parameter system of the form

$$\boldsymbol{F}(\boldsymbol{u}, \lambda, \Lambda) = \boldsymbol{f}(\boldsymbol{u}, \Lambda) - p(\lambda) = 0 \tag{2}$$

A simple and rather direct analysis would consist in successively fixing the imperfection amplitude and tracing the full fundamental path of the obtained perturbed structure in order to determine the critical states. This kind of analysis is all the more costly as only the information concerning the critical states is needed. Furthermore, it provides information only for the few amplitude values that have been fixed. In practice, it is not judicious to calculate all the different equilibrium paths. It is more advisable to determine precisely a starting critical state for given values of the additional parameters Λ, and then to follow directly the branch $\mathcal{C}$ of limit points when Λ varies. By this way, it is not necessary to compute all the equilibrium paths. Only the curve (called a fold curve) connecting the critical points is computed. This is accomplished by appending to the system of the nonlinear equilibrium equations $\boldsymbol{F}(\boldsymbol{u}, \lambda, \Lambda) = 0$ a constraint equation that characterizes the studied critical state. Doing so, the system (2) becomes an augmented system which reads

$$\boldsymbol{R}(\boldsymbol{u}, \boldsymbol{\varphi}, \lambda, \Lambda) = \begin{pmatrix} \boldsymbol{F}(\boldsymbol{u}, \lambda, \Lambda) \\ \boldsymbol{G}(\boldsymbol{u}, \boldsymbol{\varphi}, \Lambda) \end{pmatrix} = 0 \tag{3}$$

Thus, the full imperfection analysis with respect to additional parameters can be performed through two distinct steps expressed as follows :

1. On the perfect structure, for a fixed value of the extra parameters, solve the basic equilibrium problem, i.e. evaluate the fundamental path and isolate the required critical state
2. Starting from this critical state, follow the path described by the augmented system made of the basic equilibrium equations and the additional constraint equation. It has already been addressed by Jepson and Spence [1] , Wagner and Wriggers [2], and Eriksson [3] using incremental-iterative strategies.

In this paper, the imperfection analysis is reconsidered using the so called Asymptotic Numerical Method as an alternative to incremental-iterative methods. This technique which is based on high order Taylor series representations of the curves, provides crucial advantages for making the continuation of a path and detecting critical points. In Section 2, we begin with a review of the A.N.M. for tracing the fundamental path. Section 3 is devoted to the determination of a fold line using the A.N.M. concept. We make a rather general presentation of the perturbation series, of the linear system to be solved and of the specific solution procedure. More details are given in Section 4 for two kinds of imperfections : a structural geometric imperfection and a thickness imperfection. Finally, the detection of a critical state on a path is addressed in Section 5.

2 The basic equilibrium problem and the A.N.M.

The main purpose of this Section is to set the principle of the A.N.M., to outline several interesting advantages of the method over the incremental-iterative strategies and to introduce the

notations that will be used in the sequel. This method is inspired by the perturbation techniques developed by Thompson and Walker [4] and used by Noor et al. [5] for designing "reduced bases" algorithms. They have been revisited and efficiently solved by Damil and Potier Ferry [6]. A continuation method has been proposed by Cochelin and is described in detail in [7].

2.1 Basic equilibrium problem

In this Section, all the parameters are supposed to be constant, excepted the load parameter. It can be seen as a particular case of the multi-parameter problem. Assuming that the external forces $p(\lambda)$ are proportional to the external load $\boldsymbol{F}_e$, the system to solve takes the form

$$\boldsymbol{F}(\boldsymbol{u},\lambda) = \boldsymbol{f}(\boldsymbol{u}) - \lambda \boldsymbol{F}_e = 0 \tag{4}$$

where $\boldsymbol{u}$ stands for the displacement and $\boldsymbol{f}$ for the internal forces vector. At a regular point, a tangent direction $(\boldsymbol{u}_1,\lambda_1)$ is obtained from the differentiation of the residual equation (4)

$$\boldsymbol{f}_{,\boldsymbol{u}}\,.\,\boldsymbol{u}_1 - \boldsymbol{F}_e\ \lambda_1 = 0 \tag{5}$$

$\boldsymbol{f}_{,\boldsymbol{u}}$ is the tangent operator, also commonly known as the tangent stiffness operator.

2.2 A.N.M. for the calculation of the fundamental equilibrium path

2.2.1 Quadratic formulation

In the case of geometrical nonlinear elasticity, Eq. (4) is cubic with respect to $\boldsymbol{u}$. This cubic expression is not very suitable for asymptotic expansions. A quadratic expression is preferred. It is achieved by introducing the stress-strain relation as an additional equation. Eq. (4) can thus be replaced by the following equivalent system

$$\boldsymbol{F}(\boldsymbol{u},\lambda) = \left\{ \begin{array}{l} \displaystyle\int_\Omega \boldsymbol{B}^t(\boldsymbol{u})\,\boldsymbol{S}\ d\Omega - \lambda \boldsymbol{F}_e = 0 \\ \text{where}\ \ \boldsymbol{S} = \boldsymbol{D}\ \left(\boldsymbol{B}_l + \frac{1}{2}\boldsymbol{B}_{nl}(\boldsymbol{u})\right)\ \boldsymbol{u} \end{array} \right. \tag{6}$$

We have used the classical $\boldsymbol{B}$ operator defined by $\boldsymbol{B}(\boldsymbol{u})=\boldsymbol{B}_l+\boldsymbol{B}_{nl}(\boldsymbol{u})$. $\boldsymbol{S}$ is the stress operator and $\boldsymbol{D}$ is the classical elasticity operator function. The first equation stands for equilibrium. It is quadratic with respect to the set of variables $(\boldsymbol{u},\boldsymbol{S})$. The constitutive law has been introduced in order to make both equations quadratic. $\boldsymbol{B}_l$ and $\boldsymbol{B}_{nl}(\boldsymbol{u})$ are the classical operators expressing the linear and nonlinear parts of the Green-Lagrange strain [8].

2.2.2 Asymptotic expansions

Assuming that a a regular point $(\boldsymbol{u}_0,\lambda_0)$ is known, the basic idea of the A.N.M. consists in seeking the solution branch $(\boldsymbol{u},\lambda)$ in a truncated power series form with respect to a well chosen

path parameter "a". For convenience, an expansion of the variable $\boldsymbol{S}$ is also introduced, with $\boldsymbol{S}_0 = \boldsymbol{D}\,\boldsymbol{B}(\boldsymbol{u}_0)\,\boldsymbol{u}_0$

$$\begin{aligned} \boldsymbol{u}(a) &= \boldsymbol{u}_0 + a\,\boldsymbol{u}_1 + a^2\,\boldsymbol{u}_2 + \ldots + a^n\,\boldsymbol{u}_n \\ \boldsymbol{S}(a) &= \boldsymbol{S}_0 + a\,\boldsymbol{S}_1 + a^2\,\boldsymbol{S}_2 + \ldots + a^n\,\boldsymbol{S}_n \\ \lambda(a) &= \lambda_0 + a\,\lambda_1 + a^2\,\lambda_2 + \ldots + a^n\,\lambda_n \end{aligned} \tag{7}$$

Introducing these expansions into the nonlinear problem (6) and identifying the power-like terms leads to a succession of linear problems with the form

$$\text{order 1} \quad \left\{ \begin{array}{l} \displaystyle\int_\Omega \boldsymbol{B}^t(\boldsymbol{u}_0)\,\boldsymbol{S}_1 + \boldsymbol{B}^t_{nl}(\boldsymbol{u}_1)\,\boldsymbol{S}_0\;d\Omega = \lambda_1 \boldsymbol{F}_e \\ \boldsymbol{S}_1 = \boldsymbol{D}\,\boldsymbol{B}(\boldsymbol{u}_0)\,\boldsymbol{u}_1 \end{array} \right.$$

$$\text{order 2} \quad \left\{ \begin{array}{l} \displaystyle\int_\Omega \boldsymbol{B}^t(\boldsymbol{u}_0)\,\boldsymbol{S}_2 + \boldsymbol{B}^t_{nl}(\boldsymbol{u}_2)\,\boldsymbol{S}_0\;d\Omega = \lambda_2 \boldsymbol{F}_e - \int_\Omega \boldsymbol{B}^t_{nl}(\boldsymbol{u}_1)\,\boldsymbol{S}_1\;d\Omega \\ \boldsymbol{S}_2 = \boldsymbol{D}\,\boldsymbol{B}(\boldsymbol{u}_0)\,\boldsymbol{u}_2 + \frac{1}{2}\,\boldsymbol{D}\,\boldsymbol{B}_{nl}(\boldsymbol{u}_1)\,\boldsymbol{u}_1 \end{array} \right.$$

$$\vdots \qquad\qquad \vdots$$

$$\text{order } p \quad \left\{ \begin{array}{l} \displaystyle\int_\Omega \boldsymbol{B}^t(\boldsymbol{u}_0)\,\boldsymbol{S}_p + \boldsymbol{B}^t_{nl}(\boldsymbol{u}_p)\,\boldsymbol{S}_0\;d\Omega = \lambda_p \boldsymbol{F}_e - \int_\Omega \sum_{r=1}^{p-1} \boldsymbol{B}^t_{nl}(\boldsymbol{u}_r)\,\boldsymbol{S}_{p-r}\;d\Omega \\ \boldsymbol{S}_p = \boldsymbol{D}\,\boldsymbol{B}(\boldsymbol{u}_0)\,\boldsymbol{u}_p + \frac{1}{2}\,\boldsymbol{D}\displaystyle\sum_{r=1}^{p-1} \boldsymbol{B}_{nl}(\boldsymbol{u}_r)\,\boldsymbol{u}_{p-r} \end{array} \right. \tag{8}$$

Introducing the notation

$$\boldsymbol{S}^{nl}_p = \frac{1}{2}\,\boldsymbol{D}\sum_{r=1}^{p-1} \boldsymbol{B}_{nl}(\boldsymbol{u}_r)\,\boldsymbol{u}_{p-r} \tag{9}$$

the second equation of (8) can be rewritten as

$$\boldsymbol{S}_p = \boldsymbol{D}\,\boldsymbol{B}(\boldsymbol{u}_0)\,\boldsymbol{u}_p + \boldsymbol{S}^{nl}_p \tag{10}$$

The problem (8) at order p is a classical linearized elasticity problem where $\boldsymbol{S}^{nl}_p$ stands for a pre-stress term and $\int_\Omega \sum \boldsymbol{B}^t_{nl}(\boldsymbol{u}_r)\,\boldsymbol{S}_{p-r}$ for a prescribed load. There is still one unknown (λ_p) at this stage. It will disappear with the choice of "a". The path parameter "a" can be chosen such as

$$a = \frac{1}{s^2}\;\left[\;(\boldsymbol{u}-\boldsymbol{u}_0)^t\,.\,\boldsymbol{u}_1 + (\lambda-\lambda_0)\,\lambda_1\;\right] \tag{11}$$

This choice which is inspired by the arc-length continuation method identifies a as the projection of the increments $\boldsymbol{u}-\boldsymbol{u}_0$ and $\lambda-\lambda_0$ on the tangent direction. At order 1 Eq. (7) and (11) leads to

$$\boldsymbol{u}_1^t\,.\,\boldsymbol{u}_1 + \lambda_1\,\lambda_1 = s^2 \tag{12}$$

where s is a given value that fixes the length of the tangent vector. It must be noticed that it does not set the step length. This one is based on a residual criterium that will be discussed in Section 2.2.4. At order p, the relation reads

$$\boldsymbol{u}_1^t \,.\, \boldsymbol{u}_p + \lambda_1 \, \lambda_p = 0 \tag{13}$$

The system (8) and (13) uniquely determine $\boldsymbol{u}_p$, $\boldsymbol{S}_p$, λ_p.

2.2.3 Finite element method

The previous linear systems can be efficiently solved by a F.E.M. Each of these systems contains an equilibrium equation in $\boldsymbol{u}$ and $\boldsymbol{S}$ and a constitutive equation. Since classical FEM are based on a displacement formulation, it is necessary to transform the first equation into a pure displacement problem. This can be easily done by replacing the expression of $\boldsymbol{S}$ in the equilibrium. Thus, each linear problem (8) is transformed into into a pure displacement problem in $\boldsymbol{u}_p$ and a stress-strain relation which gives the stress $\boldsymbol{S}_p$. After discretization, the displacement problem at order p $(p \geq 2)$ reads

$$\begin{aligned} &\boldsymbol{K}_t \, \boldsymbol{u}_p = \lambda_p \, \boldsymbol{F}_e + \boldsymbol{F}_p^{nl} \\ &\boldsymbol{u}_1^t \, \boldsymbol{u}_p + \lambda_1 \, \lambda_p = 0 \end{aligned} \tag{14}$$

where $\boldsymbol{K}_t = \boldsymbol{K}_t(\boldsymbol{u}_0, \boldsymbol{S}_0)$ is the classical tangent stiffness matrix at the starting point $(\boldsymbol{u}_0, \lambda_0)$. $\boldsymbol{F}$ is the vector of external loads and $\boldsymbol{F}_p^{nl}$ is a load vector which depends only on the previous orders and reads

$$\boldsymbol{F}_p^{nl} = -\int_\Omega \boldsymbol{B}(\boldsymbol{u}_0) \, \boldsymbol{S}_p^{nl} - \sum_{r=1}^{p-1} \boldsymbol{B}_{nl}^t(\boldsymbol{u}_r) \, \boldsymbol{S}_{p-r} \, d\Omega \tag{15}$$

At this stage, many remarks can be made :

- All the linear systems have the same $\boldsymbol{K}_t$ matrix, hence only one matrix decomposition is required to compute the terms of the series. It allows to compute the series up to high orders (20 or 30 in practice) since the extra calculation cost consists only in the assembly of the supplementary $\boldsymbol{F}_p^{nl}$ vectors and in a back-substitution for each order.

- The problem at order 1 gives the tangent direction $(\boldsymbol{u}_1, \lambda_1)$. It corresponds to the predictor step in the incremental-iterative Newton-Raphson algorithm. The next problems can then be solved recursively since they are simple linearized elasticity problems depending on the previous orders. This algorithm is thus very easy to implement.

- The series (7) generally allows to compute a large part of the solution branch that starts at $(\boldsymbol{u}_0, \lambda_0)$ [9].

2.2.4 The continuation method

Because of the limited radius of convergence of the series, this process must be applied several times, quite in the same way as the classical continuation methods. The length of each step can

be determined by a residual criterium (see Cochelin [7]). For series truncated at order N, the maximal value of a for which the solution satisfies a requested precision ε is given by

$$a_M = \left(\frac{\varepsilon}{\| \boldsymbol{F}_{N+1}^{nl} \|} \right)^{\frac{1}{N+1}} \tag{16}$$

By applying the method from a successively updated new starting point, we can determine a complex solution branch in a step by step manner. This procedure is very robust and completely automatic from the user's point of view. Moreover, the step length is always optimal.

To illustrate the capabilities of this method , an example is provided in Fig. 2. It is a classical buckling case which involves limit points and snap-through phenomenon. The geometrical and material properties of the cylindrical panel are given in Fig. 2. For symmetry reasons, only a quarter of the panel was discretized, using a mesh with 200 triangular DKT shell elements and 726 degrees of freedom. With series truncated at order 30 and an accuracy $\varepsilon = 10^{-6}$ monitored by Eq. (16), the interesting part of the curve is fully described with only four steps.

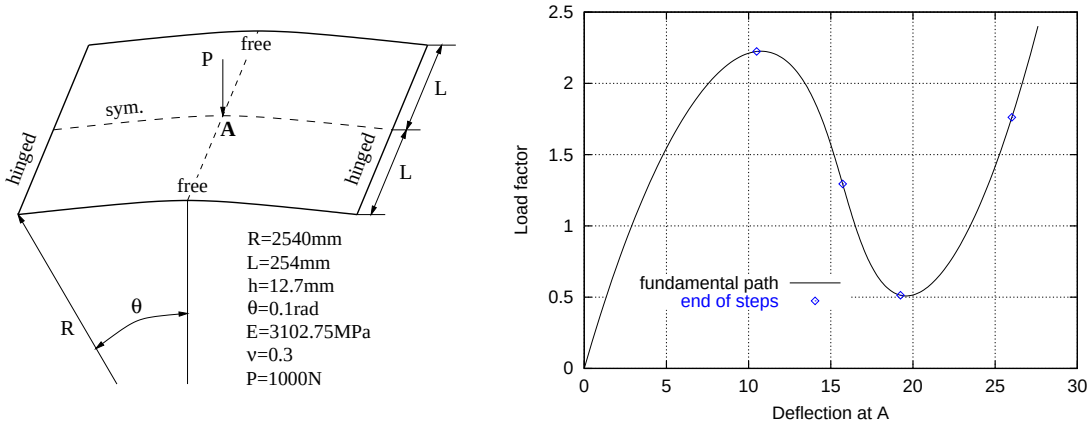

Figure 2: Cylindrical panel : problem definition and load-deflection curves for the basic equilibrium problem with series truncated at order 30 and $\varepsilon = 10^{-6}$.

3 Direct computation of critical paths

We now consider the multi-parameter nonlinear system

$$\boldsymbol{F}(\boldsymbol{u}, \lambda, \Lambda) = \boldsymbol{f}(\boldsymbol{u}, \Lambda) - p(\lambda) = 0 \tag{17}$$

We intend to compute the fold curve connecting the singular points of $\boldsymbol{F}$. To do so, additional information characterizing these singular points must be provided, yielding a so called extended or augmented system.

3.1 The augmented problem

3.1.1 The constraint equation

Many alternatives have been proposed in the literature to define the criticality, the simplest of them lying on the study of the determinant of the tangent stiffness matrix. However, this criterium is not well suited for a numerical study. The method presented here has been first introduced by Keener and Keller [], subsequently used by Moore and Spence [10], Jepson and Spence [1], and numerically investigated by Wriggers and Simo [11] and Erickson et. al [12] among others. It is based on the appearance of a null eigenvalue for the tangent operator $\boldsymbol{K}_T = \boldsymbol{F}_{,\boldsymbol{u}}$ at simple critical states. The corresponding extended system reads

$$\boldsymbol{R}\left(\boldsymbol{u},\boldsymbol{\varphi},\Lambda,\lambda\right) = \left(\begin{array}{c} \boldsymbol{F}\left(\boldsymbol{u},\Lambda,\lambda\right) \\ \boldsymbol{F}_{,\boldsymbol{u}}\left(\boldsymbol{u},\Lambda,\lambda\right)\cdot\boldsymbol{\varphi} \\ \|\boldsymbol{\varphi}\|-1 \end{array} \right) = 0 \tag{18}$$

where $\boldsymbol{\varphi}$ is the eigenvector associated with the null eigenvalue. The last normalization condition ensures its uniqueness.

For a fixed value $\Lambda = \Lambda_0$ of the additional parameters, this augmented problem gives a singular point of $\boldsymbol{F}$, either a bifurcating point or a turning point with respect to λ. When Λ varies, it provides the entire fold curve connecting the singular points of $\boldsymbol{F}$, both bifurcating or turning points with respect to λ and Λ.

3.1.2 The augmented tangent operator

Using (4), the previous system can be rewritten as

$$\boldsymbol{R}\left(\boldsymbol{u},\boldsymbol{\varphi},\Lambda,\lambda\right) = \left(\begin{array}{c} \boldsymbol{f}\left(\boldsymbol{u},\Lambda\right)-\lambda\boldsymbol{F}_e \\ \boldsymbol{f}_{,\boldsymbol{u}}\left(\boldsymbol{u},\Lambda\right)\cdot\boldsymbol{\varphi} \\ \|\boldsymbol{\varphi}\|-1 \end{array} \right) = 0 \tag{19}$$

A tangent direction $(\boldsymbol{u}_1,\boldsymbol{\varphi}_1,\Lambda_1,\lambda_1)$ is given by

$$\boldsymbol{R}_{,\boldsymbol{u}}\,.\,\boldsymbol{u}_1 + \boldsymbol{R}_{,\boldsymbol{\varphi}}\,.\,\boldsymbol{\varphi}_1 + \boldsymbol{R}_{,\Lambda}\,.\,\Lambda_1 + \boldsymbol{R}_{,\lambda}\,.\,\lambda_1 = 0 \tag{20}$$

which can be expressed as follows in a matrix form

$$\left[\begin{array}{cccc} \boldsymbol{f}_{,\boldsymbol{u}} & 0 & \boldsymbol{f}_{,\Lambda} & -\boldsymbol{F}_e \\ \boldsymbol{f}_{,\boldsymbol{u}\boldsymbol{u}}\cdot\boldsymbol{\varphi}_0 & \boldsymbol{f}_{,\boldsymbol{u}} & \boldsymbol{f}_{,\boldsymbol{u}\Lambda}\cdot\boldsymbol{\varphi}_0 & 0 \\ 0 & \boldsymbol{\varphi}_0^t & 0 & 0 \end{array} \right] \left\{ \begin{array}{c} \boldsymbol{u}_1 \\ \boldsymbol{\varphi}_1 \\ \Lambda_1 \\ \lambda_1 \end{array} \right\} = 0 \tag{21}$$

Properties concerning the regularity of $\boldsymbol{R}$ can be exhibited from the investigation of this tangent extended system, see Jepson and Spence [1], Wagner and Wriggers [2]. Recalling that all the solution points of $\boldsymbol{R}$ are singular points of $\boldsymbol{F}$, the regular points of $\boldsymbol{R}$ appear to correspond to the limit points of $\boldsymbol{F}$ with respect to λ i.e. with Λ fixed. Singular points of the extended system $\boldsymbol{R}$ can arise for $(\boldsymbol{\varphi}_0^t\,\boldsymbol{F}_e = 0\,,\ \boldsymbol{\varphi}_0^t\,(f_{,\boldsymbol{u}\boldsymbol{u}}\,\boldsymbol{\varphi}_0\,\boldsymbol{\varphi}_0) \neq 0)$ or $(\boldsymbol{\varphi}_0^t\,\boldsymbol{F}_e \neq 0\,,\ \boldsymbol{\varphi}_0^t\,(f_{,\boldsymbol{u}\boldsymbol{u}}\,\boldsymbol{\varphi}_0\,\boldsymbol{\varphi}_0) = 0)$.

3.2 Asymptotic Numerical Method

In this Section we solve the previous extended system (18) using the Asymptotic Numerical Method introduced in Section 2.2.

As previously stated, it is more convenient to turn the basic equations into a quadratic formulation in order to apply the asymptotic expansions. This stage is probably the most complex one of the procedure. The difficulty lies on the number of additional variables which need to be introduced to reduce the degree of the equations with respect to the different unknowns $\boldsymbol{u}$, $\boldsymbol{\varphi}$, λ and Λ. This procedure will be detailed in Section 4 in the cases of a geometrical shape imperfection and of a thickness imperfection. Here, we do not enter into these details. We assume that the fold line can be represented by a power series of the form

$$\begin{aligned}
\boldsymbol{u}(a) &= \boldsymbol{u}_0 + a\,\boldsymbol{u}_1 + a^2\,\boldsymbol{u}_2 + \ldots + a^n\,\boldsymbol{u}_n \\
\boldsymbol{\varphi}(a) &= \boldsymbol{\varphi}_0 + a\,\boldsymbol{\varphi}_1 + a^2\,\boldsymbol{\varphi}_2 + \ldots + a^n\,\boldsymbol{\varphi}_n \\
\lambda(a) &= \lambda_0 + a\,\lambda_1 + a^2\,\lambda_2 + \ldots + a^n\,\lambda_n \\
\Lambda(a) &= \Lambda_0 + a\,\Lambda_1 + a^2\,\Lambda_2 + \ldots + a^n\,\Lambda_n
\end{aligned} \tag{22}$$

where $(\boldsymbol{u}_0, \boldsymbol{\varphi}_0, \Lambda_0, \lambda_0)$ is supposed to be a regular initial solution point of $\boldsymbol{R}$. Replacing (22) into the nonlinear problem (18) and applying the technique described in Section 2.2 leads to the final discretized linear problem at order p

$$\begin{bmatrix} \boldsymbol{K}_T & 0 & \boldsymbol{F}_1 & -\boldsymbol{F}_e \\ \boldsymbol{K}_{\boldsymbol{\varphi}} & \boldsymbol{K}_T & \boldsymbol{F}_2 & 0 \\ 0 & \boldsymbol{\varphi}_0^t & 0 & 0 \\ \boldsymbol{u}_1^t & 0 & \Lambda_1 & \lambda_1 \end{bmatrix} \begin{bmatrix} \boldsymbol{u}_p \\ \boldsymbol{\varphi}_p \\ \Lambda_p \\ \lambda_p \end{bmatrix} = \begin{bmatrix} \boldsymbol{F}_p^{nl} \\ \boldsymbol{G}_p^{nl} \\ h_p^{nl} \\ 0 \end{bmatrix} \quad \begin{matrix} \text{size n} \\ \text{size n} \\ \text{size 1} \\ \text{size 1} \end{matrix} \tag{23}$$

The two vectors $\boldsymbol{F}_1$, $\boldsymbol{F}_2$ and the matrix $\boldsymbol{K}_{\boldsymbol{\varphi}}$ are introduced to shorten the notations. $\boldsymbol{F}_1$ and $\boldsymbol{F}_2$ stand for $f_{,\Lambda}$ and $f_{,\boldsymbol{u}\Lambda} \cdot \boldsymbol{\varphi}_0$ of Eq. (21) and $\boldsymbol{K}_{\boldsymbol{\varphi}}$ is the matrix $f_{,\boldsymbol{u}\boldsymbol{u}} \cdot \boldsymbol{\varphi}_0 = \boldsymbol{K}_{T,\boldsymbol{u}} \cdot \boldsymbol{\varphi}$. The r.h.s. vectors $\boldsymbol{F}_p^{nl}$ and $\boldsymbol{G}_p^{nl}$ and the scalar h_p^{nl} result of summations of quadratic products depending only on the solutions at previous orders. The nl subscript is used to easily distinguish this r.h.s from the other terms. The matrix $\boldsymbol{K}_{\boldsymbol{\varphi}}$ is the same whatever the imperfection. The expression of the vectors $\boldsymbol{F}_1$ and $\boldsymbol{F}_2$ and the r.h.s. depends on the type of imperfection introduced within the structure. Their expressions will be detailed in Section 4 for two types of imperfections. The last equation of the system (23) is an extended version of Eq. (13).

3.3 Procedure to solve the augmented matrix system

In practice, a gauss-like elimination is used to solve the extended system (23) in order to consider only subsystems of size n involving the $\boldsymbol{K}_T$ matrix. Such a block-elimination scheme can be found in Wriggers and Simo [11]. Its main interest relies on the fact that only the classical $\boldsymbol{K}_T$ matrix needs to be decomposed, thus saving a large amount of calculation time. The procedure presented here is inspired by this one.

Besides this particular procedure, another numerical difficulty must be pointed out. Since all the solution points of $\boldsymbol{R}$ are singular ones of $\boldsymbol{F}$, the $\boldsymbol{K}_T$ matrix is singular all along the fold line

connecting the computed solution points. That means that the classical matrix decomposition techniques cannot be used. A special procedure, based on Lagrange multipliers, is introduced to bypass this problem.

3.3.1 Block-elimination scheme at order 1

At order 1, the system (23) reads

$$\begin{bmatrix} \boldsymbol{K}_T & 0 & \boldsymbol{F}_1 & -\boldsymbol{F}_e \\ \boldsymbol{K}_{\boldsymbol{\varphi}} & \boldsymbol{K}_T & \boldsymbol{F}_2 & 0 \\ 0 & \boldsymbol{\varphi}_0^t & 0 & 0 \\ \boldsymbol{u}_1^t & 0 & \Lambda_1 & \lambda_1 \end{bmatrix} \begin{bmatrix} \boldsymbol{u}_1 \\ \boldsymbol{\varphi}_1 \\ \Lambda_1 \\ \lambda_1 \end{bmatrix} = \begin{bmatrix} 0 \\ 0 \\ 0 \\ s^2 \end{bmatrix} \tag{24}$$

Premultiplying the first equation of (23) by $\boldsymbol{\varphi}_0^t$ yields a compatibility relation between Λ_1 and λ_1

$$\Lambda_1 = c_1\,\lambda_1 \quad \text{with} \;\; c_1 = \frac{\boldsymbol{\varphi}_0^t\,\boldsymbol{F}_e}{\boldsymbol{\varphi}_0^t\,\boldsymbol{F}_1} \tag{25}$$

Replacing Eq. (25) in the first equation of (23) leads to the linear system

$$\boldsymbol{K}_T\,\boldsymbol{u}_1 = \lambda_1\,\boldsymbol{h}_1 \quad \text{with} \;\; \boldsymbol{h}_1 = \boldsymbol{F}_e - c_1\,\boldsymbol{F}_1 \tag{26}$$

It can be noticed that the vector $\boldsymbol{h}_1$ is orthogonal to $\boldsymbol{\varphi}_0$. Because of the singularity of $\boldsymbol{K}_T$, the linear system (26) is solved as follows. The solution vector is decomposed into its projection on $\boldsymbol{\varphi}_0$ and its orthogonal part

$$\boldsymbol{u}_1 = \alpha\,\boldsymbol{\varphi}_0 + \lambda_1\,\boldsymbol{v}_1^{\perp}\,, \quad \alpha \in \mathbb{R},\; \boldsymbol{\varphi}_0^t\,\boldsymbol{v}_1^{\perp} = 0 \tag{27}$$

The orthogonality condition is then enforced through the use of a Lagrange multiplier μ and the orthogonal part of u_1 is obtained by

$$\begin{bmatrix} \boldsymbol{K}_T & \boldsymbol{\varphi}_0 \\ \boldsymbol{\varphi}_0^t & 0 \end{bmatrix} \begin{bmatrix} \boldsymbol{v}_1^{\perp} \\ \mu \end{bmatrix} = \begin{bmatrix} \boldsymbol{h}_1 \\ 0 \end{bmatrix} \tag{28}$$

Introducing Eq. (27) in the second equation of (23) and premultiplying by $\boldsymbol{\varphi}_0^t$ yields another compatibility relation [1]

$$\alpha = c_2\,\lambda_1 \quad \text{with} \;\; c_2 = -\frac{c_1\,\boldsymbol{\varphi}_0^t\boldsymbol{F}_2 + \boldsymbol{\varphi}_0^t\,\boldsymbol{K}_{\boldsymbol{\varphi}}\boldsymbol{v}_1^{\perp}}{\boldsymbol{\varphi}_0^t\,\boldsymbol{K}_{\boldsymbol{\varphi}}\boldsymbol{\varphi}_0} \tag{29}$$

replacing this expression in the second equation of (23) leads to

$$\boldsymbol{K}_T\,\boldsymbol{\varphi}_1 = \lambda_1\,\boldsymbol{h}_2 \tag{30}$$

[1] The assumed regularity of $\boldsymbol{R}$ at the starting point ensures that that the denominators of c_1 and c_2 are not null. Indeed, they exactly correspond to $\boldsymbol{\varphi}_0^t\,(f_{,\boldsymbol{uu}}\,\boldsymbol{\varphi}_0\,\boldsymbol{\varphi}_0)$ and $\boldsymbol{\varphi}_0^t\,\boldsymbol{f}_{,\Lambda}$ (see e.g. Wagner and Wriggers [2]).

where

$$\boldsymbol{h}_2 = c_2\,\boldsymbol{K}_{\boldsymbol{\varphi}}\boldsymbol{\varphi}_0 - \boldsymbol{K}_{\boldsymbol{\varphi}}\boldsymbol{v}_1^{\perp} - c_1\,\boldsymbol{F}_2\ , \quad \boldsymbol{\varphi}_0^t\,\boldsymbol{h}_2 = 0 \tag{31}$$

Again, the solution vector $\boldsymbol{\varphi}$ is decomposed into

$$\boldsymbol{\varphi}_1 = \beta\,\boldsymbol{\varphi}_0 + \lambda_1\,\boldsymbol{p}_1^{\perp}\ , \quad \beta \in \mathbb{R},\ \boldsymbol{\varphi}_0^t\,\boldsymbol{p}_1^{\perp} = 0 \tag{32}$$

with the orthogonal part $\boldsymbol{p}_1^{\perp}$ obtained by

$$\begin{bmatrix} \boldsymbol{K}_T & \boldsymbol{\varphi}_0 \\ \boldsymbol{\varphi}_0^t & 0 \end{bmatrix} \begin{bmatrix} \boldsymbol{p}_1^{\perp} \\ \mu \end{bmatrix} = \begin{bmatrix} \boldsymbol{h}_2 \\ 0 \end{bmatrix} \tag{33}$$

Then, the third equation of (23) gives

$$\beta = 0 \tag{34}$$

and the fourth equation provides an expression for λ_1. At this stage, the terms at order 1 are fully determined

$$\begin{aligned} \lambda_1 &= \frac{s}{\sqrt{d}} \qquad \text{with } \ d = 1 + c_1^2 + c_2^2 + \boldsymbol{v}_1^{\perp\,t}\boldsymbol{v}_1^{\perp} \\ \Lambda_1 &= c_1\,\lambda_1 \\ \boldsymbol{u}_1 &= c_2\,\boldsymbol{\varphi}_0 + \lambda_1\,\boldsymbol{v}_1^{\perp} \\ \boldsymbol{\varphi}_1 &= \lambda_1\,\boldsymbol{p}_1^{\perp} \end{aligned} \tag{35}$$

3.3.2 Block-elimination scheme at order p

The resolution is slightly different than before because of the r.h.s. terms of the system (23). Nevertheless, the block-elimination procedure remains the same. That is why the resolution will not be detailed here. Despite the additional r.h.s. terms, the global calculation cost remains the same. Indeed, the solutions can be expressed as the sum of a term which is proportional to the solutions at order 1 and a term which come from the new r.h.s. vectors. As a result, only two system resolutions are needed to compute all the terms at order p.

4 Two specific types of imperfections

In section 2.2.1, emphasis has been put on the fact that the transformation of the governing equations into a quadratic form was crucial for the asymptotic expansions. The main purpose of this section is to provide a general procedure for the obtaining of such a formulation. This procedure is based on the introduction of well chosen extra variables, thus augmenting the number of equations to be solved but reducing the degree of each of the governing equations. This required procedure does not restrict the range of problems which can be treated by the A.N.M. It is detailed here for two common types of imperfections. The expression of the vectors $\boldsymbol{F}_1$, $\boldsymbol{F}_2$, $\boldsymbol{F}_p^{nl}$ and $\boldsymbol{G}_p^{nl}$ of the discretized augmented system (23) will also be given for each studied case.

4.1 Geometrical shape imperfection

A simplified structure with a geometrical shape imperfection $\boldsymbol{u}^\star$ is presented in Fig. 3. The black color is used for the perfect structure in its initial state, the green color denotes the imperfect structure in its initial state and the blue color indicates the imperfect structure in its deformed state.

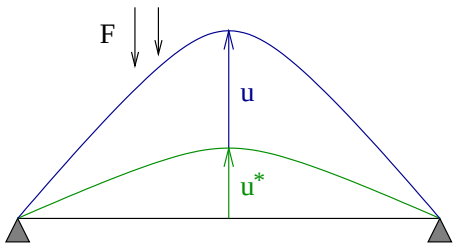

Figure 3: Structure with a geometrical shape imperfection

The strain $\boldsymbol{\gamma}$ of the deformed imperfect structure is deduced from

$$\boldsymbol{\gamma}(\boldsymbol{u},\boldsymbol{u}^\star) = \boldsymbol{\gamma}(\boldsymbol{u}+\boldsymbol{u}^\star) - \boldsymbol{\gamma}(\boldsymbol{u}^\star) \tag{36}$$

where $\boldsymbol{\gamma}$ is the classical Green Lagrange strain defined as

$$\boldsymbol{\gamma}(\boldsymbol{u}) = \frac{1}{2}(\nabla\boldsymbol{u} + \nabla^t\boldsymbol{u}) + \frac{1}{2}(\nabla\boldsymbol{u}\,\nabla^t\boldsymbol{u}) = \boldsymbol{\gamma}^l(\boldsymbol{u}) + \boldsymbol{\gamma}^{nl}(\boldsymbol{u},\boldsymbol{u}) \tag{37}$$

Combined with (37), (36) becomes

$$\boldsymbol{\gamma}(\boldsymbol{u},\boldsymbol{u}^\star) = \boldsymbol{\gamma}^l(\boldsymbol{u}) + \boldsymbol{\gamma}^{nl}(\boldsymbol{u},\boldsymbol{u}) + 2\,\boldsymbol{\gamma}^{nl}(\boldsymbol{u},\boldsymbol{u}^\star) \tag{38}$$

Compared to the classical expression (37) of the strain, there is a new term $\boldsymbol{\gamma}^{nl}(\boldsymbol{u},\boldsymbol{u}^\star)$ which is bilinear with respect to $\boldsymbol{u}$ and $\boldsymbol{u}^\star$. In order to get a scalar extra parameter, the imperfection is written as

$$\boldsymbol{u}^\star = \eta\,\boldsymbol{u}_0^\star \tag{39}$$

where $\boldsymbol{u}_0^\star$ is a fixed displacement which gives the shape of the imperfection and η is its amplitude. Using the notations introduced in Section 2, the governing equations can then be expressed as

$$\boldsymbol{F}(\boldsymbol{u},\eta,\lambda) = \left\{ \begin{array}{l} \displaystyle\int_\Omega \boldsymbol{B}^t(\boldsymbol{u})\,\boldsymbol{S} + \eta\,\boldsymbol{B}_{nl}^t(\boldsymbol{u}_0^\star)\,\boldsymbol{S}\;d\Omega - \lambda\boldsymbol{F}_e = 0 \\ \quad \boldsymbol{S} = \boldsymbol{D}\;\left(\boldsymbol{B}_l + \frac{1}{2}\boldsymbol{B}_{nl}(\boldsymbol{u}) + \eta\,\boldsymbol{B}_{nl}(\boldsymbol{u}_0^\star)\right)\,\boldsymbol{u} \end{array} \right. \tag{40}$$

and the constraint equation reads

$$\boldsymbol{F}_{,\boldsymbol{u}}\,(\boldsymbol{u},\eta,\lambda)\cdot\boldsymbol{\varphi} = \left\{ \begin{array}{l} \displaystyle\int_\Omega \boldsymbol{B}^t(\boldsymbol{u})\,\boldsymbol{\Psi} + \eta\,\boldsymbol{B}_{nl}^t(\boldsymbol{u}_0^\star)\,\boldsymbol{\Psi} + \boldsymbol{B}_{nl}^t(\boldsymbol{\varphi})\,\boldsymbol{S}\;d\Omega = 0 \\ \quad \boldsymbol{\Psi} = \boldsymbol{D}\;\left(\boldsymbol{B}_l + \boldsymbol{B}_{nl}(\boldsymbol{u}) + \eta\,\boldsymbol{B}_{nl}(\boldsymbol{u}_0^\star)\right)\,\boldsymbol{\varphi} \end{array} \right. \tag{41}$$

where $\boldsymbol{\Psi}$ is the stress associated with the null eigenvector $\boldsymbol{\varphi}$. Eq. (40) is quadratic with respect to the variable set $(\boldsymbol{u}, \boldsymbol{S}, \eta, \lambda)$ and (41) is quadratic with respect to $(\boldsymbol{u}, \boldsymbol{S}, \boldsymbol{\varphi}, \boldsymbol{\Psi}, \eta, \lambda)$.

The next step consists in developing each of the variables in a power series form. Introducing the mixed variable $\boldsymbol{U} = \{\boldsymbol{u}, \boldsymbol{S}, \boldsymbol{\varphi}, \boldsymbol{\Psi}, \eta, \lambda\}^t$, the series expansion reads

$$\boldsymbol{U}(a) = \boldsymbol{U}_0 + a\,\boldsymbol{U}_1 + a^2\,\boldsymbol{U}_2 + \ldots + a^n\,\boldsymbol{U}_n \tag{42}$$

where $(\boldsymbol{u}_0, \boldsymbol{S}_0, \boldsymbol{\varphi}_0, \boldsymbol{\Psi}_0, \eta_0, \lambda_0)$ is supposed to be a regular initial solution point. The introduction of the series into (40) and (41) leads at order p $(p \geq 2)$ to

$$\left\{\begin{array}{l} \displaystyle\int_\Omega \tilde{\boldsymbol{B}}_0^t\,\boldsymbol{S}_p + \boldsymbol{B}_{nl}^t(\boldsymbol{u}_p)\,\boldsymbol{S}_0 + \eta_p\,\boldsymbol{B}_{nl}^t(\boldsymbol{u}_0^\star)\,\boldsymbol{S}_0\;d\Omega = \lambda_p \boldsymbol{F}_e - \int_\Omega \sum_{r=1}^{p-1} \boldsymbol{B}_{nl}^t(\boldsymbol{u}_r + \eta_r\,\boldsymbol{u}_0^\star)\,\boldsymbol{S}_{p-r}\;d\Omega \\ \quad \boldsymbol{S}_p = \boldsymbol{D}\,\left(\tilde{\boldsymbol{B}}_0\,\boldsymbol{u}_p + \eta_p\,\boldsymbol{B}_{nl}(\boldsymbol{u}_0)\,\boldsymbol{u}_0^\star\right) + \boldsymbol{S}_p^{nl} \\ \displaystyle\int_\Omega \tilde{\boldsymbol{B}}_0^t\,\boldsymbol{\Psi}_p + \boldsymbol{B}_{nl}^t(\boldsymbol{\varphi}_p)\,\boldsymbol{S}_0 + \boldsymbol{B}_{nl}^t(\boldsymbol{u}_p)\,\boldsymbol{\Psi}_0 + \eta_p\,\boldsymbol{B}_{nl}^t(\boldsymbol{u}_0^\star)\,\boldsymbol{\Psi}_0 + \eta_p\,\boldsymbol{B}_{nl}^t(\boldsymbol{\varphi}_0)\,\boldsymbol{S}_p\;d\Omega \\ \qquad\qquad = -\displaystyle\int_\Omega \sum_{r=1}^{p-1} \boldsymbol{B}_{nl}^t(\boldsymbol{\varphi}_r)\,\boldsymbol{S}_{p-r}\;d\Omega - \int_\Omega \sum_{r=1}^{p-1} \boldsymbol{B}_{nl}^t(\boldsymbol{u}_r + \eta_r\,\boldsymbol{u}_0^\star)\,\boldsymbol{\Psi}_{p-r}\;d\Omega \\ \quad \boldsymbol{\Psi}_p = \boldsymbol{D}\,\left(\tilde{\boldsymbol{B}}_0\,\boldsymbol{\varphi}_p + \boldsymbol{B}_{nl}(\boldsymbol{\varphi}_0)\,(\boldsymbol{u}_p + \eta_p\,\boldsymbol{u}_0^\star)\right) + \boldsymbol{\Psi}_p^{nl} \end{array}\right. \tag{43}$$

$\tilde{\boldsymbol{B}}_0$ has been introduced to shorten the notations and stands for $\boldsymbol{B}(\boldsymbol{u}_0 + \eta_0\,\boldsymbol{u}_0^\star)$. Because of the introduction of the imperfection, the expressions of $\boldsymbol{S}_p^{nl}$ and $\boldsymbol{\Psi}_p^{nl}$ are slightly more complicated than in Section 2.2. They will not been detailed here. In order to perform an F.E.M., $\boldsymbol{S}_p$ and $\boldsymbol{\Psi}_p$ are replaced in the the equilibrium and the constraint equations. After discretization, it yields the two following displacement problems

$$\begin{array}{l} \boldsymbol{K}_t\,\boldsymbol{u}_p + \eta_p\,\boldsymbol{F}_1 = \lambda_p\,\boldsymbol{F} + \boldsymbol{F}_p^{nl} \\ \boldsymbol{K}_{\boldsymbol{\varphi}}\,\boldsymbol{u}_p + \boldsymbol{K}_T\,\boldsymbol{\varphi}_p + \eta_p\,\boldsymbol{F}_2 = \boldsymbol{G}_p^{nl} \end{array} \tag{44}$$

where $\boldsymbol{K}_t = \boldsymbol{K}_t\,(\boldsymbol{u}_0 + \eta_0 \boldsymbol{u}_0^\star, \boldsymbol{S}_0)$ is the tangent stiffness matrix at the starting point $(\boldsymbol{u}_0, \eta_0, \lambda_0)$. The vectors $\boldsymbol{F}_p^{nl}$ and $\boldsymbol{G}_p^{nl}$ depend only on the previous orders. They can easily be inferred from (43). The expressions of the two vectors $\boldsymbol{F}_1$ and $\boldsymbol{F}_2$ depend on the type of imperfection. In the present case, they read

$$\begin{array}{l} \boldsymbol{F}_1 = \displaystyle\int_\Omega \left(\tilde{\boldsymbol{B}}_0^t\,\boldsymbol{D}\,\boldsymbol{B}_{nl}(\boldsymbol{u}_0) + \boldsymbol{G}^t\,\hat{\boldsymbol{S}}_0\,\boldsymbol{G}\right)\,\boldsymbol{u}_0^\star\;d\Omega \\ \boldsymbol{F}_2 = \displaystyle\int_\Omega \left(\tilde{\boldsymbol{B}}_0^t\,\boldsymbol{D}\,\boldsymbol{B}_{nl}(\boldsymbol{\varphi}_0) + \boldsymbol{B}_{nl}(\boldsymbol{\varphi}_0)\,\boldsymbol{D}\,\boldsymbol{B}_{nl}(\boldsymbol{u}_0) + \boldsymbol{G}^t\,\hat{\boldsymbol{\Psi}}_0\,\boldsymbol{G}\right)\,\boldsymbol{u}_0^\star\;d\Omega \end{array} \tag{45}$$

The matrices $\hat{\boldsymbol{S}}_0$ and $\hat{\boldsymbol{\Psi}}_0$ contain components of the stress vectors $\boldsymbol{S}_0$ and $\boldsymbol{\Psi}_0$, and $\boldsymbol{G}$ is the gradient matrix of the shape functions.

Two additional equations are yet missing. The first one is the normalization condition on $\boldsymbol{\varphi}$. It is exactly the same than in the general case. The second one fixes the path parameter "a" of the fold line. It is chosen such as

$$\boldsymbol{u}_1^t\,\boldsymbol{u}_p + \eta_1\,\eta_p + \lambda_1\,\lambda_p = 0 \tag{46}$$

Putting together these two additional equations and the system (44) yields an augmented system with the same form as (23). The procedure introduced in Section 3.3 can then be used to solve it.

4.2 Thickness imperfection

Taking a thickness imperfection into account is more complex. Indeed, it depends on the type of finite element used for the analysis. In this section, the study will be carried out with the DKT18 shell element. Its description can be found in []. In the formulation of this element, the thickness h appear only in the elasticity matrix $\boldsymbol{D}$ which is given by

$$\boldsymbol{D} = \begin{bmatrix} \dfrac{E\,h}{1-\nu^2}\begin{bmatrix} 1 & 1 & 0 \\ 1 & 1 & 0 \\ 0 & 0 & \dfrac{1-\nu}{2} \end{bmatrix} & 0 \\ 0 & \dfrac{E\,h^3}{12(1-\nu^2)}\begin{bmatrix} 1 & 1 & 0 \\ 1 & 1 & 0 \\ 0 & 0 & \dfrac{1-\nu}{2} \end{bmatrix} \end{bmatrix} \tag{47}$$

The tensile part of $\boldsymbol{D}$ is linear with respect to h and the bending part is cubic. $\boldsymbol{D}$ can thus be rewritten as

$$\boldsymbol{D} = \boldsymbol{D}^1\,h + \boldsymbol{D}^3\,h^3 \tag{48}$$

According to (37) and (48), the constitutive law $\boldsymbol{S}{=}\boldsymbol{D}\,\boldsymbol{\gamma}(\boldsymbol{u})$ is quadratic with respect to $\boldsymbol{u}$ and cubic with respect to h. Some additional variables need to be introduced in order to reduce the order of the equations and to turn them into a quadratic form. This is achieved as follows

$$\boldsymbol{F}(\boldsymbol{u},h,\lambda) = \begin{cases} \displaystyle\int_\Omega \boldsymbol{B}^t(\boldsymbol{u})\,\boldsymbol{S}\;d\Omega - \lambda\boldsymbol{F}_e = 0 \\ \boldsymbol{S} = \boldsymbol{D}\,\boldsymbol{\gamma} \\ \boldsymbol{\gamma} = \left(\boldsymbol{B}_l + \frac{1}{2}\boldsymbol{B}_{nl}(\boldsymbol{u})\right)\,\boldsymbol{u} \\ \boldsymbol{D} = D^1\,h + \boldsymbol{D}^3\,eh \\ e = h^2 \end{cases} \tag{49}$$

Through the introduction of $\boldsymbol{S}$, the equilibrium equation becomes quadratic. Then, $\boldsymbol{D}$ is made quadratic with respect to h and the additional variable e. The constitutive equation is quadratic in $\boldsymbol{D}$ and $\boldsymbol{\gamma}$. In this way, each equation of the previous system is quadratic. It will significantly

reduce the number of products to form when introducing the series. The same work is done with the constraint equation by adding the variables $\boldsymbol{\Psi}$ and $\boldsymbol{\varepsilon}$.

$$\boldsymbol{F}_{,\boldsymbol{u}}\,(\boldsymbol{u},h,\lambda)\cdot\boldsymbol{\varphi}=\left\{\begin{array}{c}\displaystyle\int_\Omega \boldsymbol{B}^t(\boldsymbol{u})\,\boldsymbol{\Psi}+\boldsymbol{B}^t_{nl}(\boldsymbol{\varphi})\,\boldsymbol{S}\;d\Omega=0\\ \boldsymbol{\Psi}=\boldsymbol{D}\,\boldsymbol{\varepsilon}\\ \boldsymbol{\varepsilon}=(\boldsymbol{B}_l+\boldsymbol{B}_{nl}(\boldsymbol{u}))\;\boldsymbol{\varphi}\\ \boldsymbol{D}=\boldsymbol{D}^1\,h+\boldsymbol{D}^3\,eh\\ e=h^2\end{array}\right. \tag{50}$$

Each of the variables is then expanded into a power series form which can be expressed as

$$\boldsymbol{U}(a)=\boldsymbol{U}_0+a\,\boldsymbol{U}_1+a^2\,\boldsymbol{U}_2+\ldots+a^n\,\boldsymbol{U}_n \tag{51}$$

where the mixed variable $\boldsymbol{U}$ stands for $\{\boldsymbol{u},\boldsymbol{S},\boldsymbol{\gamma},\boldsymbol{\varphi},\boldsymbol{\Psi},\boldsymbol{\varepsilon},\boldsymbol{D},e,h,\lambda\}^t$., and the term $\boldsymbol{U}_0$ refers to a regular starting solution point. Introducing the development (51) into the systems (49) and (50) and identifying the power-like terms provides the expressions of the additional variables at order p $(p\geq 2)$

$$\begin{array}{c}e_p=2h_0h_p+e_p^{nl}\\ \boldsymbol{\gamma}_p=\boldsymbol{B}(\boldsymbol{u}_0)\,\boldsymbol{u}_p+\boldsymbol{\gamma}_p^{nl}\\ \boldsymbol{\varepsilon}_p=\boldsymbol{B}(\boldsymbol{u}_0)\,\boldsymbol{\varphi}_p+\boldsymbol{B}_{nl}(\boldsymbol{\varphi}_0)\,\boldsymbol{u}_p+\boldsymbol{\varepsilon}_p^{nl}\end{array} \tag{52}$$

where the terms with the nl subscript involve products at previous orders. Using the expression of e_p and introducing the notation $\tilde{\boldsymbol{D}}$ leads to

$$\boldsymbol{D}_p=(\boldsymbol{D}^1+3h_0^2\,\boldsymbol{D}^3)\,h_p+\boldsymbol{D}_p^{nl}=\tilde{\boldsymbol{D}}\,h_p+\boldsymbol{D}_p^{nl} \tag{53}$$

The equilibrium and the constraint equations and their associated constitutive equations can be expressed at the order p using the previous expressions. The additional variables are then eliminated in order to keep only the variables $\boldsymbol{u}$ and h. In fact, they have been useful only because they have made the series expansion procedure easier. The remaining equations read

$$\left\{\begin{array}{l}\displaystyle\int_\Omega \boldsymbol{B}^t(\boldsymbol{u}_0)\,\boldsymbol{S}_p+\boldsymbol{B}^t_{nl}(\boldsymbol{u}_p)\,\boldsymbol{S}_0\;d\Omega=\lambda_p\boldsymbol{F}_e-\int_\Omega\sum_{r=1}^{p-1}\boldsymbol{B}^t_{nl}(\boldsymbol{u}_r)\,\boldsymbol{S}_{p-r}\;d\Omega\\ \boldsymbol{S}_p=\boldsymbol{D}_0\,\boldsymbol{B}(\boldsymbol{u}_0)\,\boldsymbol{u}_p+\tilde{\boldsymbol{D}}\,\boldsymbol{B}(\boldsymbol{u}_0)\,\boldsymbol{u}_0\,h_p+\boldsymbol{S}_p^{nl}\\ \displaystyle\int_\Omega \boldsymbol{B}^t(\boldsymbol{u}_0)\,\boldsymbol{\Psi}_p+\boldsymbol{B}^t_{nl}(\boldsymbol{\varphi}_p)\,\boldsymbol{S}_0+\boldsymbol{B}^t_{nl}(\boldsymbol{u}_p)\,\boldsymbol{\Psi}_0\;d\Omega\\ \qquad\qquad=-\displaystyle\int_\Omega\sum_{r=1}^{p-1}\boldsymbol{B}^t_{nl}(\boldsymbol{\varphi}_r)\,\boldsymbol{S}_{p-r}\;d\Omega-\int_\Omega\sum_{r=1}^{p-1}\boldsymbol{B}^t_{nl}(\boldsymbol{u}_r)\,\boldsymbol{\Psi}_{p-r}\;d\Omega\\ \boldsymbol{\Psi}_p=\boldsymbol{D}_0\,\boldsymbol{B}(\boldsymbol{u}_0)\,\boldsymbol{\varphi}_p+\boldsymbol{D}_0\,\boldsymbol{B}_{nl}(\boldsymbol{\varphi}_0)\,\boldsymbol{u}_p+\tilde{\boldsymbol{D}}\left(\boldsymbol{B}(\boldsymbol{u}_0)\,\boldsymbol{\varphi}_0+\boldsymbol{B}_{nl}(\boldsymbol{\varphi}_0)\,\boldsymbol{u}_0\right)h_p+\boldsymbol{\Psi}_p^{nl}\end{array}\right. \tag{54}$$

After a F.E.M. discretization, this corresponding matrix system reads

$$\begin{aligned} \boldsymbol{K}_t\,\boldsymbol{u}_p + h_p\,\boldsymbol{F}_1 &= \lambda_p\,\boldsymbol{F}_e + \boldsymbol{F}_p^{nl} \\ \boldsymbol{K}_{\boldsymbol{\varphi}}\,\boldsymbol{u}_p + \boldsymbol{K}_T\,\boldsymbol{\varphi}_p + h_p\,\boldsymbol{F}_2 &= \boldsymbol{G}_p^{nl} \end{aligned} \tag{55}$$

$$\begin{aligned} \boldsymbol{F}_1 &= \int_\Omega \boldsymbol{B}^t(\boldsymbol{u}_0)\,\tilde{\boldsymbol{D}}\,\boldsymbol{B}(\boldsymbol{u}_0)\,\boldsymbol{u}_0\;d\Omega \\ \boldsymbol{F}_2 &= \int_\Omega \boldsymbol{B}^t(\boldsymbol{u}_0)\,\tilde{\boldsymbol{D}}\,\boldsymbol{B}(\boldsymbol{u}_0)\,\boldsymbol{\varphi}_0 + \boldsymbol{B}^t(\boldsymbol{u}_0)\,\tilde{\boldsymbol{D}}\,\boldsymbol{B}_{nl}(\boldsymbol{\varphi}_0)\,\boldsymbol{u}_0 + \boldsymbol{B}_{nl}^t(\boldsymbol{\varphi}_0)\,\tilde{\boldsymbol{D}}\,\boldsymbol{B}(\boldsymbol{u}_0)\,\boldsymbol{u}_0\;d\Omega \end{aligned} \tag{56}$$

Augmented with the two additional equations related to the normalization of $\boldsymbol{\varphi}$ and the path parameter a, the system (55) can be recursively solved using the procedure introduced in Section 3.3.

5 Detection of critical states on the equilibrium path

Before following the fold curve, a starting limit point must be precisely detected on the fundamental path. Standard methods for determining such a singular point have been presented in Section 3.1.1. The method presented here consists in detecting the critical states by the mean of a perturbed equilibrium problem that will be subsequently solved with the A.N.M. It has been first introduced by Boutyour [13] and used by Vannucci et al. [14].

5.1 The bifurcation indicator

The singular point is searched on the equilibrium path defined by (17) for given values Λ_0 of the additional parameters which define the initial imperfection. The resulting governing equation

$$\boldsymbol{F}(\boldsymbol{u}, \Lambda_0, \lambda) = \boldsymbol{f}(\boldsymbol{u}, \Lambda_0) - p(\lambda) = 0 \tag{57}$$

can be seen as a particular case of the basic equilibrium problem (4). Thus, the procedure given in Section 2 can be applied for the calculation of the equilibrium path.

The detection of the criticality is made through the introduction of a perturbation into the system. This perturbed problem is described by

$$\boldsymbol{f}_{,\boldsymbol{u}}\,.\,\boldsymbol{\Delta u} = \Delta\mu\,\boldsymbol{f}_e \tag{58}$$

where $\boldsymbol{\Delta u}$ is the displacement response of the structure to the load perturbation $\Delta\mu\,\boldsymbol{f}_e$. Focusing on the evolution of $(\boldsymbol{\Delta u}, \Delta\mu\,\boldsymbol{f})$ while following the fundamental path, a critical state can be characterized as follows

i) It is a point on the fundamental path where the tangent operator $\boldsymbol{K}_T = \boldsymbol{f}_{,\boldsymbol{u}}$ is singular. Standard methods are based on this criterium.

ii) For a fixed load perturbation $\Delta\mu$, it is the point where the displacement response $\boldsymbol{\Delta u}$ tends to infinity. Because of these infinite values of the displacement, this criterium is not suitable for a numerical use.
iii) For a fixed displacement perturbation $\boldsymbol{\Delta u}$, it is the point where the load response $\Delta\mu$ tends to zero. When $\boldsymbol{\Delta u}$ is fixed, $\Delta\mu$ can be seen as a stiffness measurement.

The last criterium will be used here. Hence, the singular points correspond to the null values of the bifurcation indicator $\Delta\mu$. The system (58) consists of n equations and involves $n+1$ unknowns, the n components of $\boldsymbol{\Delta u}$ and $\Delta\mu$. An additional condition must be provided for (58) to admit a unique solution for each regular point of the fundamental path. Since we have decided to fix the displacement perturbation rather than the load perturbation, this condition will be chosen such as

$$\|\boldsymbol{\Delta u}\| = 1 \tag{59}$$

Equations (58) and (59) form a well-posed system which will be solved using the A.N.M.

5.2 Determination of the bifurcation indicator with the A.N.M.

We assume that an analytical expression of the equilibrium path has been obtained using the procedure of Section 2

$$\begin{aligned} \boldsymbol{u}(a) &= \boldsymbol{u}_0 + a\,\boldsymbol{u}_1 + a^2\,\boldsymbol{u}_2 + \ldots + a^n\,\boldsymbol{u}_n \\ \lambda(a) &= \lambda_0 + a\,\lambda_1 + a^2\,\lambda_2 + \ldots + a^n\,\lambda_n \end{aligned} \tag{60}$$

The perturbations $\boldsymbol{\Delta u}$ and $\Delta\mu$ are then developed with regard to the same parameter a

$$\begin{aligned} \boldsymbol{\Delta u}(a) &= \boldsymbol{\Delta u}_0 + a\,\boldsymbol{\Delta u}_1 + a^2\,\boldsymbol{\Delta u}_2 + \ldots + a^n\,\boldsymbol{\Delta u}_n \\ \Delta\mu(a) &= \Delta\mu_0 + a\,\Delta\mu_1 + a^2\,\Delta\mu_2 + \ldots + a^n\,\Delta\mu_n \end{aligned} \tag{61}$$

where $\boldsymbol{\Delta u}_0$ is the response of the structure to the perturbation at the starting point $(\boldsymbol{u}_0, \lambda_0)$. After the introduction of these series into Eq. (58) and (59) and with the F.E.M. notations introduced in Section 2.2.3, the linear system to solve at order p $(p \geq 1)$ reads

$$\begin{aligned} \boldsymbol{K}_t\,\boldsymbol{\Delta u}_p &= \Delta\mu_p\,\boldsymbol{f}_e + \boldsymbol{\Delta F}_p^{nl} \\ \boldsymbol{\Delta u}_0^t\,\boldsymbol{\Delta u}_p &= \sum_{r=1}^{p-1} \boldsymbol{\Delta u}_r\,\boldsymbol{\Delta u}_{p-r} = \alpha_p \end{aligned} \tag{62}$$

The vectors $\boldsymbol{\Delta F}_p^{nl}$ depend only on $\boldsymbol{u}_r$ and $\boldsymbol{\Delta u}_r$ at previous order. Here, these $\boldsymbol{u}_r$ terms and the tangent stiffness matrix $\boldsymbol{K}_T$ are exactly the same as those previously calculated in Section 2 for the fundamental path. As a result, this procedure can extremely easily be superposed on the algorithm for the fundamental path. The extra calculation cost lies in the assembly of the $\boldsymbol{\Delta F}_p^{nl}$ vectors, the calculation of the scalars α_p and the resolution of a few linear systems with a $\boldsymbol{K}_T$ matrix already decomposed.

The critical points correspond to the values a_c of the parameter a for which $\Delta\mu(a)$ is zero and the corresponding critical load is obtained by $\lambda(a_c)$. It must be noticed that this procedure does not only provide the critical load. The associated eigenvector is also given by $\boldsymbol{\Delta u}(a_c)$. As a result, all the initial information that is required for the calculation of the fold curve of Section 3 is supplied by this procedure. Moreover, the numerical precision of this information can be monitored through the use of a residual criterium in order to satisfy a given precision ε. A very accurate starting point for the fold curve can thus be obtained.

5.3 A numerical example : the cylindrical panel

The example presented in Fig. 4 demonstrates the capabilities of this algorithm to detect singular points as well as limit points. The geometry of the panel is the same as in Fig. 2, excepted for the thickness which is now $h = 6.35mm$. This value leads to a far more complicated equilibrium path. One half of the panel was discretized in order to get the bifurcated path. For symmetry reasons, it does not appear if only one quarter is considered. Series were truncated at order 30. Two limit points and two bifurcation points, connected by a bifurcated path, were detected. Both singular points and their associated eigenmodes were obtained with a required accuracy $\varepsilon = 10^{-8}$. Any of the limit point can then be used as a starting point for the computation of the fold curve, as described in Section 3.

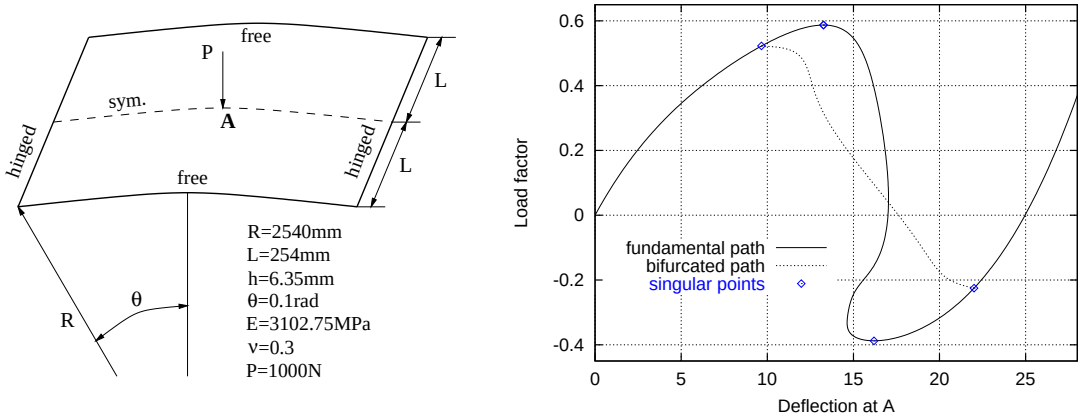

Figure 4: Cylindrical panel : problem definition and detected singular points on the fundamental path of the basic equilibrium problem

6 Conclusions

References

[1] A. Jepson, A. Spence. *Folds in solutions of two parameter systems and their calculation. Part I*. SIAM J. Numer. Anal., 22, (1985), 347-368.

[2] W. Wagner, P. Wriggers. *Calculation of bifurcation points via fold curves*. In W. Wagner, P. Wriggers (eds.), *Nonlinear Computational Mechanics*. Springer-Verlag, Berlin Heidelberg (1991), 69-84.

[3] A. Eriksson. *Equilibrium subsets for multi-parametric structural analysis*. Comput. Methods Appl. Mech. Engrg., 140, (1997), 305-327.

[4] J. Thompson, A. Walker. *The nonlinear perturbation analysis of discrete structural systems*. Int. J. Solids Structures, 4, (1968), 757-758.

[5] A. Noor, J. Peters. *Reduced basis technique for nonlinear analysis of structures*. AIAA Journal - N4, 18, (1980), 455-462.

[6] N. Damil, M. Potier-Ferry. *A new method to compute perturbed bifurcations: application to the buckling of imperfect elastic structures*. International Journal of Engineering Sciences - N9, 28, (1990), 943-957.

[7] B. Cochelin. *A path following technique via an asymptotic numerical method*. Computers & Structures, 29, (1994), 1181-1192.

[8] M. Crisfield. *Nonlinear Finite Element Analysis of Solids ans Structures, Vol.2*. John Wiley and Sons, 1st edn. (1997).

[9] B. Cochelin, N. Damil, M. Potier-Ferry. *The Asymptotic-Numerical-Method: an efficient perturbation technique for nonlinear structural mechanics*. Revue Européenne des Eléments Finis, 3, (1994), 281-297.

[10] G. Moore, A. Spence. *The calculation of turning points of nonlinear equations*. SIAM J. Numer. Anal., 17, (1980), 567-576.

[11] P. Wriggers, J. Simo. *A general procedure for the direct calculation of turning and bifurcation points*. Int. J. Numer. Meth. Eng., 30, (1990), 155-176.

[12] A. Eriksson, C. Pacoste, A. Zdunek. *Numerical Analysis of complex instability behaviour using incremental-iterative strategies*. Comput. Methods Appl. Mech. Engrg., 179, (1999), 265-305.

[13] E. Boutyour. *Détection des bifurcations par des méthodes asymptotiques-numériques*. In *Deuxième colloque national en calcul des structures*, vol. 2. Giens, France (May 1995).

[14] P. Vannucci, B. Cochelin, N. Damil, M. Potier-Ferry. *An asymptotic-numerical method to compute bifurcating branches*. Int. J. Numer. Meth. Eng., 41, (1998), 1365-1389.